Modeling and sliding mode control of a DFIG fueled by a three-level PWM cascade application to wind energy

Naim. Cherfia, Djallel. Kerdoun

Abstract— In this paper, we study the control of active and reactive power for a doubly fed induction generator (DFIG) using sliding mode control (SMC) method feeding by inverter a three – level structure NPC for variable speed wind energy. We first present the dynamic model of DFIG connected by wind turbine and grid system, then we modeling and control strategy of inverter three-level structure NPC. Finally, we will prove that the inverter three-level PWM which allows the minimizing of harmonics stator current and wide linear modulation range and ameliorate the quality of energy injected into the electricity grid.

Index Terms—turbine, DFIG, SMC, 3L-PWM

I. Introduction

Nowadays, disadvantages of different traditional central for electricity generation using fossil fuels (coal, oil, natural gas ..), through the use of energy called "renewable" (wind power and solar). The latter is fully in the global effort to reduce CO2 emissions.

Wind power is clear prominently, not replace conventional sources, but as an additional extra energy to nuclear energy. A wind turbine has the role of converting kinetic energy of the wind into electrical energy.

Currently, the wind system with variable speed based on Doubly Fed Induction Generator (DFIG) is the most used on farms onshore wind. Its main advantage, not least, is to have its three-phase static converters designed for a portion of nominal power of the DFIG, making it an important economic benefit compared to other solutions Possible conversion of electromechanical (synchronous machine with permanent magnets for example). Indeed, DFIG allows operation over a range of ± 30% speed around synchronous speed, thus guaranteeing reduced dimensions of the static converters because they are connected between the rotor coil of the DFIG and the electrical network.

The proposed control by sliding mode can be applied to the control of active and reactive power generated by the DFIG in a wind energy conversion system and the possibility of improving the quality of electrical energy and suppress low level harmonics supplied to the network by the three-level converter structure NPC.

The authors are with the LGEC – Research Laboratory, Department of Electrical Engineering, Constantine 1 University, 25000 Constantine, Algeria. Emails: msn822009@live.fr, kerdjallel@yahoo.fr

II. Kinetic energy of wind - Conversion into Mechanical Energy

Consider the horizontal axis wind turbine system shown in figure (Fig. 1.) which shows wind speed V_1 upstream of the wind turbine and the speed V_2 downstream.

Assuming that the wind speed through the rotor is equal to the average between the undisturbed speed of the wind V_1 before and after the speed of wind passing through the wind rotor V_2 whether $\frac{V_1+V_2}{2}$, the mass of moving air density ρ through the surface S blade in one second is:

$$m=\frac{\rho s\left(V_1+V_2\right)}{2} \tag{1}$$

Power P_m then extracted is expressed by half the product of mass and the reduction of wind speed (Newton's second law):

$$P_m=\frac{m\left(V_1^2-V_2^2\right)}{2} \tag{2}$$

Either by replacing m by its expression in (2):

$$P_m=\frac{\rho s\left(V_1+V_2\right)\left(V_1^2-V_2^2\right)}{4} \tag{3}$$

Undisturbed winds theoretically pass through the same surface S without decrease speed, is the speed V_1, power P_{mt} corresponding would then be:

$$P_{mt}=\frac{\rho s V_1^2}{2} \tag{4}$$

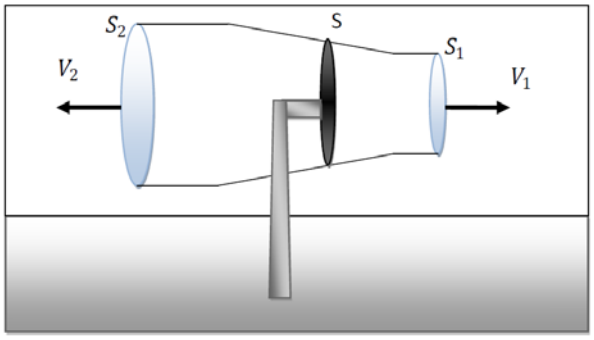

Figure.1.Stream tube around a wind turbine

The ratio between the power extracted from the wind and the total power theoretically available is:

$$\frac{P_m}{P_{mt}} = \frac{\left(1+\left(\frac{V_2}{V_1}\right)\right)\left(1-\left(\frac{V_2}{V_1}\right)^2\right)}{2} \quad (5)$$

it can be noticed that the ratio $\frac{P_m}{P_{mt}}$ also called power coefficient C_p which has a maximum of 16/27 or 0.59.

The model is based on the characteristics of steady state power of the turbine [1],[2],[3].

$$P_m = \frac{P_m}{P_{mt}} P_{mt} = C_p \cdot P_{mt} = \frac{1}{2} \cdot C_p(\lambda) \cdot \rho \cdot \pi \cdot R^2 \cdot V_1^3 \quad (6)$$

With

$$\lambda = \frac{\Omega_1 \cdot R}{V_1} \quad (7)$$

Ω_1: Rotation speed before multiplier.
R: rotor radius 35.25 m.
ρ: air density,1.225 kg.m^{-3}.

$$C_P = f(\lambda,\beta) = C_p\left(\frac{C_1}{\lambda_i} - C_3\beta - C_4\right)\exp\left(\frac{C_5}{\lambda_i}\right) + C_6\lambda \quad (8)$$

With:

$$\frac{1}{\lambda_i} = \frac{1}{\lambda + 0.08\beta} - \frac{0.035}{\beta^3 + 1}$$

C1=0.5176; C2=116; C3=0.4; C4=5; C5=21; C6=0.0068 [1], [2], [3].

Characteristics of Cp in terms of λ for different values of the pitch angle are shown in Fig.2. The maximum value of Cp (Cpmax=0.4353) is reached of β=2° and λ=10.01. This particular value of λ is defined as the nominal value [3], [4].

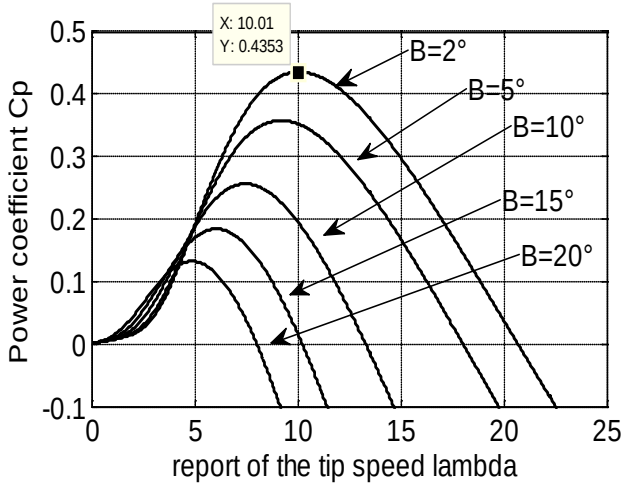

Figure.2. The power factor for different angles of stalls.

III. Dynamic Model of the Doubly Fed Induction Generator

A model always used for the doubly fed induction generator (DFIG) is the model of Park. The electrical equations of the DFIG by reference in the Park are given as follows[5],[6],[7].

$$\begin{cases} V_{sd} = R_s i_{sd} + \dfrac{d\varphi_{sd}}{dt} - \omega_s \varphi_{sq} \\ V_{sq} = R_s i_{sq} + \dfrac{d\varphi_{sq}}{dt} + \omega_s \varphi_{sd} \end{cases} \quad (9)$$

$$\begin{cases} V_{rd} = R_r i_{rd} + \dfrac{d\varphi_{rd}}{dt} - \omega_r \varphi_{rq} \\ V_{rq} = R_r i_{rq} + \dfrac{d\varphi_{rq}}{dt} + \omega_r \varphi_{rd} \end{cases} \quad (10)$$

The electromagnetic torque is expressed as:

$$C_{em} = p\left(\varphi_{sd} \cdot i_{sq} - \varphi_{sq} \cdot i_{sd}\right) \quad (11)$$

Stator and rotor variables are both referred to the stator reference Park frame. With the following orientation, the d component of the stator flux is equal to the total flux whereas the q component of the stator flux is null Fig. 3.

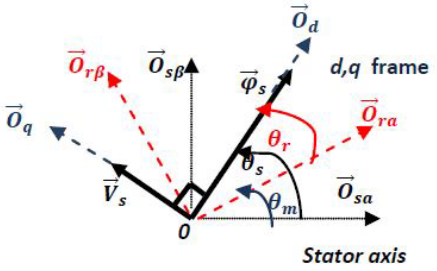

Figure.3. Determination of the electrical angles in Park reference frame.

$$\varphi_{sd} = \varphi_s, \varphi_{sq} = 0 \quad (12)$$

the electromagnetic torque can be given as follows:

$$C_{em} = -p\frac{L_m}{L_s} i_{rq} \varphi_{sd} \quad (13)$$

Assuming that the resistance of the stator winding R_s is neglected, and referring to the chosen reference frame, the voltage equations and the flux equations of the stator winding can be simplified in steady state as follows[8],[9]:

$$\begin{cases} V_{sd} = 0 \\ V_{sq} = V_s + \omega_s \varphi_s \end{cases} \quad (14)$$

$$\begin{cases} \varphi_{sd} = L_s i_{sd} + L_m i_{rd} \\ 0 = L_s i_{sq} + L_m i_{rq} \end{cases} \quad (15)$$

From (15), the equations linking the stator currents to the rotor currents are deduced below:

$$\begin{cases} i_{sd} = \dfrac{\varphi_s}{L_s} - \dfrac{L_m}{L_s} i_{rd} \\ i_{sq} = -\dfrac{L_m}{L_s} i_{rq} \end{cases} \quad (16)$$

The active and reactive powers at the stator side are defined as:

$$\begin{cases} P_s = V_{sd} i_{sd} + V_{sq} i_{sq} \\ Q_s = V_{sq} i_{sd} - V_{sd} i_{sq} \end{cases} \quad (17)$$

Taking into consideration the chosen reference frame, the above power equations can be written as follows:

$$\begin{cases} P_s = V_s i_{sq} \\ Q_s = V_s i_{sd} \end{cases} \quad (18)$$

Replacing the stator currents by their expressions given in

(10), the equations below are obtained:

$$\begin{cases} P_s = -V_s \dfrac{L_m}{L_s} i_{rq} \\ Q_s = \dfrac{V_s \varphi_s}{L_s} - \dfrac{V_s L_m}{L_s} i_{rd} \end{cases} \quad (19)$$

The block diagram of the DFIG model in Park reference frame is depicted in Fig 4, assuming a constant stator voltage (v_s).

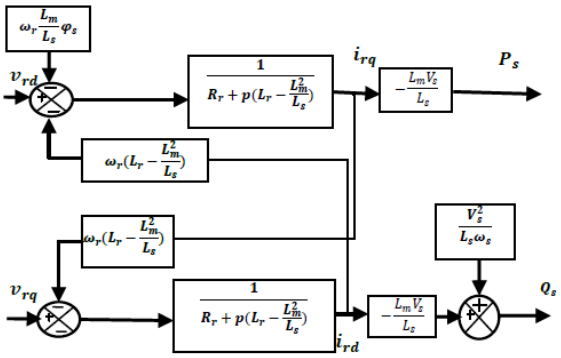

Figure 4. Block diagram of the DFIG model.

IV. Math Sliding Mode Control (SMC)

A sliding mode controller (SMC) is a Variable Structure Controller (VSC). Basically, a VSC includes several different continuous functions that can map plant state to a control surface, whereas switching among different functions is determined by plant state represented by a switching function. The design of control system will be demonstrated for a following nonlinear system [10], [11], [12]:

$$\dot{X} = f(x,t) + B(x,t) \cdot u(x,t) \quad (20)$$

Where $X \in R^n$ is the state vector,$(X,t \notin R^n$, $B(X,t) \in R^{n.m}$, $U \in Rn$, is the control vector.

From the system (20), it possible to define a set S of the state trajectories x such as:

$$S = \{X(t) | S(X,t) = 0\} \quad (21)$$

Where:

$$S(X,t) = [S_1(X,t), S_2(X,t), S_3(X,t), \cdots \cdots \cdots, S(X,t)]^T \quad (22)$$

And []T denotes the transposed vector, S is called the sliding surface.

To bring the state variable to the sliding surfaces, the following two conditions have to be satisfied:

$$S(X,t) = 0, \dot{S}(X,t) = 0 \quad (23)$$

The control law satisfies the precedent conditions is presented in the following form:

$$\begin{cases} U_{dq} = U_{eq} + U_n \\ U_n = -K_f \cdot sign(S(X,t)) \end{cases} \quad (24)$$

Where Udq is the control vector, Ueq is the equivalent control vector, Un is the switching part of the control (the correction factor), Kf is the controller gain. Ueq can be obtained by considering the condition for the sliding regime, S(X,t) The equivalent control keeps the state variable on sliding surface, once they reach it. For the defined function [13], [14]:

$$sign(\varphi) = \begin{cases} 1, if & \varphi \rangle 0 \\ 0, if & \varphi = 0 \\ -1, if & \varphi \langle 0 \end{cases} \quad (25)$$

The controller described by (24) presents high robustness, insensitive to parameter fluctuations and disturbances, but it will have high-frequency switching (chattering phenomena) near the sliding surface due to sign function involved by introducing a boundary layer with width [15].

In (24) we have:

$$U_{dq} = U_{eq} - K_f \cdot sign(S(X,t)) \quad (26)$$

Consider a Lyapunov function:

$$V = \frac{1}{2} S(X,t)^2 \quad (27)$$

If the Lyapunov theory of stability is used to ensure that SMC is attractive and invariant, In this document, we are using the sliding surface proposed by J.J. Slotine [16] [17]:

the following condition has to be satisfied:

$$\dot{V} = \frac{1}{2} \frac{d}{dt} S(X,t)^2 \le 0 \quad (28)$$

In this paper, we use the sliding surface proposed by J.J. Slotine [16] [17]:

$$S(X) = \left(\frac{\partial}{\partial t} + \lambda_x \right)^{n-1} e(x) \quad (29)$$

Where e(x) is the error vector (e(x)=X*-X), λx is a positive coefficient, n is the system order.

V. Application of SMC to DFIG

The rotor currents (which are linked to active and reactive powers by equation (19), quadrature rotor current i_{qr} linked to stator active power Ps and direct rotor current i_{dr} linked to stator reactive power Q_s) have to track appropriate current references, so, a sliding mode control based on the above Park reference frame is used.

we can obtain the sliding surfaces representing the error between the measured and references rotor currents as follow:

$$\begin{cases} \dot{S}_d = \dot{i}_{dr}^* - \left(\dfrac{V_{dr}}{\sigma L_r} - \dfrac{R_r}{\sigma L_r} i_{dr} + \omega_r i_{qr} \right) \\ \dot{S}_q = \dot{i}_{qr}^* - \left(\dfrac{V_{qr}}{\sigma L_r} - \dfrac{R_r}{\sigma L_r} i_{qr} - \omega_r i_{qr} + \dfrac{M}{\sigma L_r L_s} \varphi_s \omega_r \right) \end{cases} \quad (30)$$

V_{dr} and V_{qr} will be the two components of the control vector used to constraint the system to converge to S_{sq}=0. The control vector U_{eq} is obtain by imposing $\dot{S}_{dq}$ so the equivalent control components are given by the following relation:

$$U_{eq} = \begin{bmatrix} L_r \sigma \dot{i}_{dr}^* + R_r i_{dr} - L_r \sigma \omega_r i_{qr} \\ L_r \sigma \dot{i}_{qr}^* + R_r i_{qr} + L_r \sigma \omega_r i_{dr} - s \dfrac{M}{L_s} V_s \end{bmatrix} \quad (31)$$

VI. Modelisation of PWM three-level inverter NPC

Figure 5 shows the structure of a PWM inverter three-level NPC structure. We begin by defining the connection function F_{ki} of the switch. It is 1 if the switch is closed and 0 otherwise[18],[19].

In controllable mode, the inverter connection functions are linked by relation (32).

$$\begin{cases} F_{k1} = 1 - F_{k4} \\ F_{k2} = 1 - F_{K3} \end{cases} \quad (32)$$

With, k = 1 , 2 or 3 , represents the number of arms.

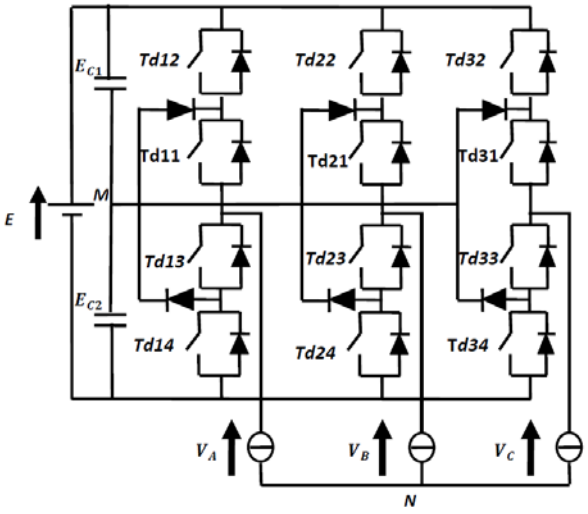

Figure 5. Three-level inverter with NPC structure

We define the connection function F_{km}^{b} the half-arms as follows:

$$\begin{cases} F_{k1}^{b} = F_{k1} \times F_{k2} \\ F_{k0}^{b} = F_{k3} \times F_{k4} \end{cases} \quad (33)$$

We denote by: m = 1: the half upper arm and m = 0 : the half-arm down.

The potentials of the nodes A, B and C of inverter PWM three levels, by relation to point M is expressed as follows[18],[19]:

$$\begin{cases} V_{AM} = F_{11}^{b} \times U_{C1} - F_{10}^{b} \times U_{C2} \\ V_{BM} = F_{21}^{b} \times U_{C1} - F_{10}^{b} \times U_{C2} \\ V_{CM} = F_{31}^{b} \times U_{C1} - F_{30}^{b} \times U_{C2} \end{cases} \quad (34)$$

The simple voltages of output are written:

$$\begin{bmatrix} V_A \\ V_B \\ V_C \end{bmatrix} = \frac{1}{3} \begin{bmatrix} 2 & -1 & -1 \\ -1 & 2 & -1 \\ -1 & -1 & 2 \end{bmatrix} \times \left\{ \begin{bmatrix} F_{11}^{b} \\ F_{21}^{b} \\ F_{31}^{b} \end{bmatrix} U_{C1} \begin{bmatrix} F_{10}^{b} \\ F_{20}^{b} \\ F_{31}^{b} \end{bmatrix} U_{C2} \right\} \quad (36)$$

VII. Regulation With Buckle of Power

To improve the control system the DFIG, we will introduce an additional loop control of active and reactive power in the block diagram of the control loop without power so that each axis controller contains two PI-SMC control, one to control the power and the other rotor current (Fig. 6) .

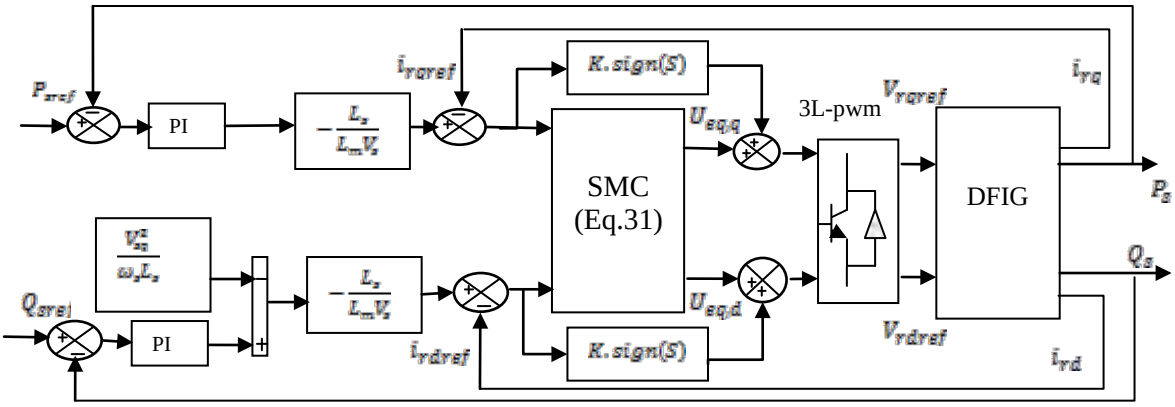

Figure 6. Schema block indirect regulation with SMC.

VIII. Simulation Results:

The simulation is done by imposing active and reactive powers references (P_{ref}, Q_{ref}), While the DFIG is driven at variable speed P_{ref} varies between -300000 and -1000000 watts and Q_{ref}=0 var and Isabc varies between 1000A and 2500A

with:

The simulation results are given by the following figures.

Figure 7 present two bipolar saw tooth caries the inverter 3L-PWM and the figures 8 and 9 present the simple voltage Va and this specter of a three-phase inverter 3L-pwm.

Figure 10 present the stator active power and its reference profiles injected into the grid using 3L-PWM.

The stator reactive power and its reference profiles using 3L-PWM is presented in Fig.11.

Fig.12 show the stator current using 3L-PWM.

Fig. 13 show the harmonic spectrum of output phase stator current obtained using Fast Fourier Transform (FFT) technique for 3L-PWM inverter. It can be clear observed that all the lower order harmonics are reduced for 3L-PWM inverter (THD = 0.2074 %).

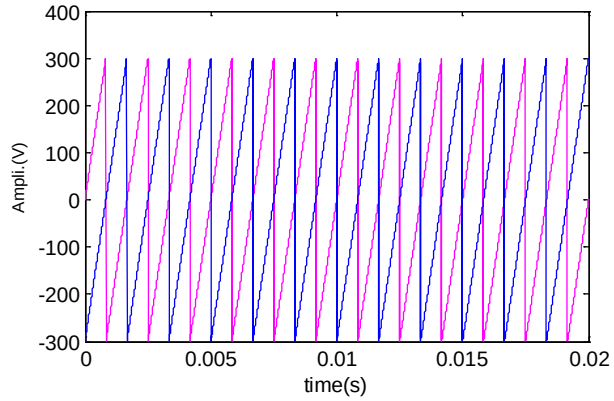

Figure 7. Two bipolar Saw tooth caries the inverter 3L-PWM

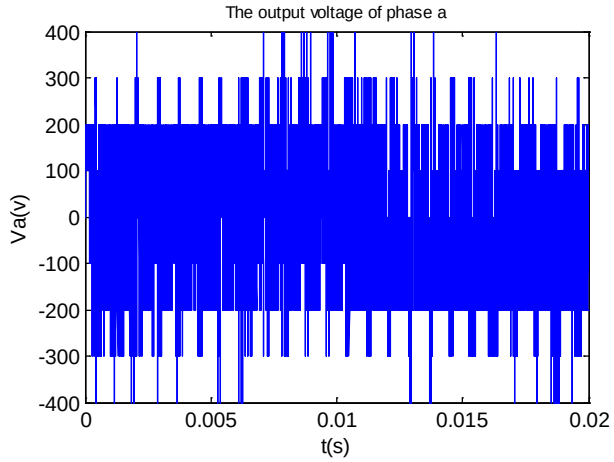

Figure 8.The simple voltage Va of a three-phase inverter 3L-pwm.

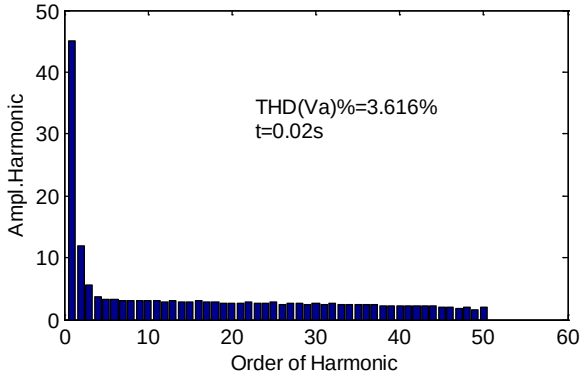

Figure 9.THD of the voltage Va with 3L-pwm

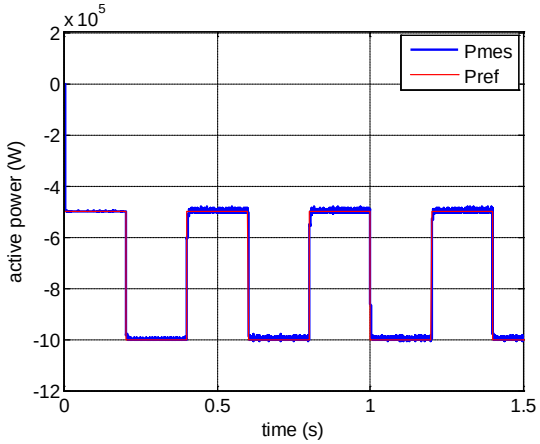

Figure 10. Electrical active power produced with SMC control using 3L-pwm.

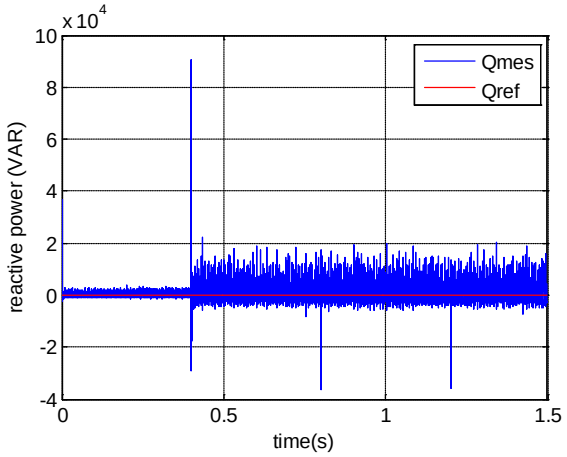

Figure 11. Electrical reactive power produced with SMC control using 3L-pwm.

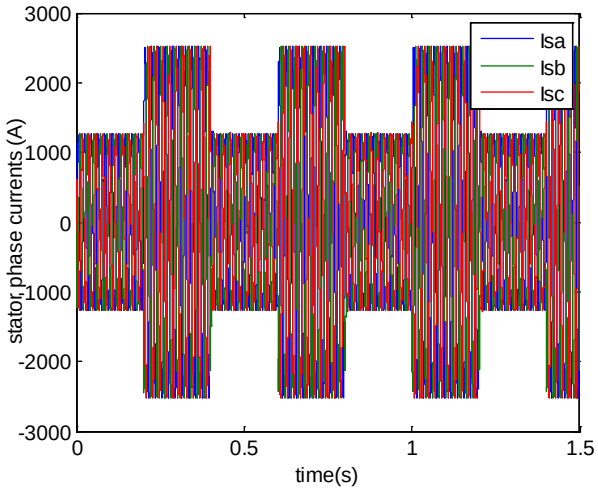

Figure 12. Stator phase currents with SMC control using 3L-pwm.

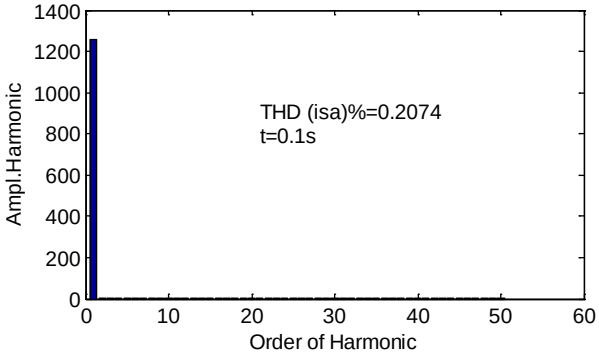

Figure 13. THD of current Isa with SMC control using 3L-pwm.

IX. Conclusion

In our work, we have established the model of the generator using its power equations in the dq axis system related to synchronization. We have also presents simulation results of sliding mode control for active and reactive indirect power control of a DFIG, using the modulation strategy of 3L-PWM technique. The DFIG active and reactive power control with SMC using 3L-PWM technique had good performance it is clear in the spectrum of phase stator current harmonics which the use of the 3L-PWM, it is minimized of harmonics.

APPENDIX A

- Nominal Power =1.5(Mw)
- Stator Per Phase Resistance =0.012 (Ω)
- Rotor Per Phase Resistance=0.021 (Ω)
- Stator Leakage Inductance= $2.0372.10^{-004}$ (H)
- Rotor Leakage Inductance= $1.7507.10^{-004}$ (H)
- Magnetizing Inductance= 0.0135 (H)
- Number Of Poles Pairs=2
- Moment Of Inertia= 1000 ($Kg.M^2$)
- Friction Coefficient =0.0024

REFERENCES

[1] Lubosny, Wind Turbine Operation in Electric Power Systems, Berlin, Germany: Springer, 2003.

[2] Hugo, E. M. L. (2007). Maximum Power Tracking Control Scheme For Wind Generator Systems, Thesis of Master, University of Texas, December 2007.

[3] V. Perelmuter, Electrotechnical Systems: Simulation with Simulink® and SimPowerSystems™. CRC Press, 2012. (Book)

[4] S. Heier, "Gid Integration of Wind Energy Conversion Systems". England: John Wiley & Sons, 1998.

[5] S. El Aimani, "Modélisation de Différentes Technologies d'Eoliennes Intégrées dans un Réseau de Moyenne Tension", *Thèse de Doctorat. Ecole Centrale de Lille et Université des Sciences et Technologies de Lille 1*, Décembre 2004. (These in French)

[6] F. Poitiers, "Etude et Commande de Génératrice Asynchrone pour l'Utilisation de l'Energie Eolienne", *Thèse de Doctorat. Université de Nantes*, Décembre 2003. (These in French)

[7] D. Kairus, R. Wamkeue, B.Belmadani and M. Benghanem, "Variable structure control of DFIG for wind power generatin and harmonic current mitigatin", *AECE*, Vol. 10, N°. 4, 2010. (Article)

[8] A. Gaillard , P. Poure , S. Saadate , M. Machmoumc, "Variable speed DFIG wind energy system for power generation and harmonic current mitigation", *Renewable Energy*, Vol. 34, Issue 6, PP 1545-1553, June 2009. (Article)

[9] M. Boutoubat, L. Mokrani, M. Machmoum, "Control of a wind energy conversion system equipped by a DFIG for active power generation and power quality improvement", *Renewable Energy*, Vol. 50, PP 378-386, February 2013. (Article)

[10] J. Lo, Y. Kuo", "Decoupled fuzzy sliding mode control", *IEEE Trans. Fuzzy Syst*, Vol. 6, N°. 3, pp. 426-435, 1998. (Article)

[11] Nasri A, Hazzab A, Bousserhane IK, Hadjiri S, Sicard P, "Two wheel speed robust sliding mode control for electrical vehicle drive", *Serbian J Electr Eng*, Vol. 5, N°. 2, 199–216, November 2008. (Article)

[12] D. Kairous, R. Wamkeue, "DFIG-based fuzzy sliding-mode control of WECS with a flywhhell energy storage", *Electric Power Systems Research*, Vol. 93, PP 16-23, December 2012. (Article)

[13] Bekakra Y, Ben Attous D, "Sliding mode controls of active and reactive power of a DFIG with MPPT for variable speed wind energy conversion", *Aust J Basic Appl Sci*, Vol. 5, N°. 12, 2274–2286, 2011. (Article)

[14] Y. Bekakra, D. Ben attous, "Direct control of doubly fed induction generator fed by PWM converter with a variable structure control based on a sliding mode control", *International Journal of System Assurance Engineering and Management, Springer*, Vol. 5, Issue 3, pp. 213-218, September 2014. (Article)

[15] A. Mezouar, M.K. Fellah, S. Hadjeri, "Adaptive sliding mode observer for induction motor using two-time-scale approach", *Electric Power Systems Research (Elsevier)*, DOI:10.1016/ j.epsr. 2006.05.010, 2006. (Article)

[16] J. Slotine, W. Li, Applied non-linear Control. Prentice-Hall Edition, 1991. (Book)

[17] M. Abid, A. Mansouri, A. Aissaoui, B. Belabbes, "Sliding mode application in position control of an induction machine", *J. Electr. Engin*, Vol. 59, N°. 6, pp. 322-327, 2008. (Article)

[18] T. Abdelkrim, E. Berkouk, K. Aliouane, K. Benamrane, and T. Benslimane, "Etude et réalisation d'un onduleur à trois niveaux commandé par MLI vectorielle," *Revue des Energies Renouvelables*, vol. 14, pp. 211-217, 2011. (Article)

[19] D. Beriber, A. Talha, F. Bouchafaa, M. Boucherit, and E. Berkouk, "Modelling and Control of a Power Electronic Cascade for the Multi DC Bus Supply of a Three-Level NPC VSI." (Article)